Magnetic structure of CuO by neutron diffraction with polarization analysis

1992 J. Phys.: Condens. Matter 4 5327

(http://iopscience.iop.org/0953-8984/4/23/009)

J. Phys.: Condens. Matter 4 (1992) 5327–5338. Printed in the UK

Magnetic structure of CuO by neutron diffraction with polarization analysis

M Aïn†, A Menelle†, B M Wanklyn†‡ and E F Bertaut§

† Laboratoire Léon Brillouin (CEA–CNRS), CEN-Saclay, 91191 Gif sur Yvette Cédex, France

‡ Clarendon Laboratory, Parks Road, Oxford OX1 3PU, UK

§ Laboratoire de Cristallographie (CNRS), 166X, 38042 Grenoble Cédex, France

Received 22 July 1991, in final form 24 February 1992

Abstract. Neutron diffraction with polarization analysis was performed on a single crystal of CuO, oriented with its a^* and c^* axes in the diffraction plane. It was verified that in the commensurate phase I (0–212.7 K; $k = (\frac{1}{2}, 0, -\frac{1}{2})$), the magnetic moments were indeed along b^*, but it was found that in the incommensurate phase II (212.7–232.5 K; $k = (0.506, 0, -0.483)$) there also exists a component of the magnetic moment along b^* in disagreement with an earlier study by Forsyth *et al.*

Our data are in agreement with the very recent results of Brown *et al.* We propose a helimagnetic arrangement in the incommensurate phase II, with the magnetic moments rotating in the plane $(b^*; 0.506a^* + 1.517c^*)$. We present here a short account of our experimental results, a study of the stability of the magnetic structure in phase II and the symmetry analysis of the possible magnetic space groups.

1. Introduction

The interplay between superconductivity and magnetism in HTSC copper oxides has encouraged investigations on magnetic materials containing Cu–O–Cu bonds. A variety of these bonds are realized in the apparently simple cupric oxide CuO (tenorite), belonging to the monoclinic space group $C2/c$ (No 15). To our knowledge, Forsyth *et al* (1988), Aïn *et al* (1989) and Yang *et al* (1988, 1989) have previously studied the structure or the dynamics of the spin system in this compound.

The crystalline structure of CuO has been refined by Åsbrink and Norrby (1970) from x-ray data, and some of their results are summarized in table 1 and in figure 1.

CuO is an insulating material; its unit cell is shown in figure 1. It contains four Cu–O groups. Each copper ion is located on a centre of symmetry and is nearly rectangularly coordinated by four oxygen ions, forming a CuO_4 plate. The non-primitive translation of the space group $C = [\frac{1}{2}, \frac{1}{2}, 0]$ connects the copper ions so as to form ribbons of side-sharing CuO_4 plates, stretching along [110]. Conversely each oxygen ion is enclosed in a tetrahedron of copper ions; it is located on a twofold axis, hence generating ribbons along $[1\bar{1}0]$. As a consequence, we have two copper sites labelled Cu_I and Cu_{II} (one on each set of ribbons) that are connected via the symmetry axis.

Inside the copper tetrahedron, there are six Cu–O–Cu angles, of which only four are different owing to the presence of the twofold axis. It is accepted since the

0953-8984/92/235327+12$04.50

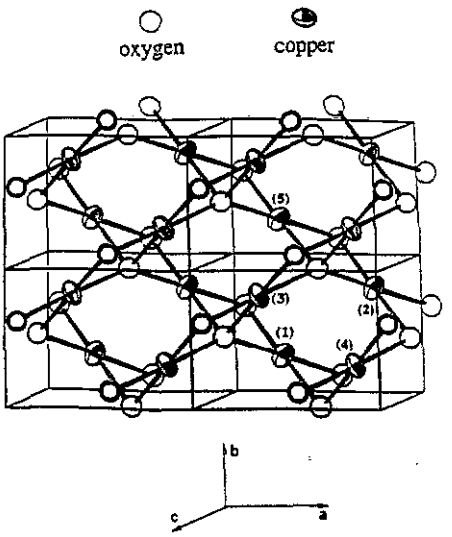

Figure 1. Perspective view showing four cells of CuO. The spheres are oxygen ions, and the ellipsoids are copper ions; the ions are fatter from front to back. One can recognize ribbons of CuO_4 adjacent plates along [110] and [$\bar{1}$10]. The numbers in parentheses distinguish the different copper ions cited in table 1 and in the text.

Table 1. Crystallographic information on CuO from Åsbrink and Norrby (1970): (room temperature)

(i) CuO; space group, $C2/c$ (No 15).
(ii) $a = 4.6837 \pm 5$ Å, $b = 3.4226 \pm 5$ Å, $c = 5.1288 \pm 6$ Å and $\beta = 99.54 \pm 1°$.
(iii) Cu on 4(c): $[(\frac{1}{4}, \frac{1}{4}, 0); (1)]$; $[(\frac{3}{4}, \frac{3}{4}, 0); (2)]$; $[(\frac{1}{4}, \frac{3}{4}, \frac{1}{2}); (3)]$; $[(\frac{3}{4}, \frac{1}{4}, \frac{1}{2}); (4)]$.
(iv) O on 4(e): $[(0, y, \frac{1}{4}); (1)]$; $[(\frac{1}{2}, \frac{1}{2}+y, \frac{1}{4}); (2)]$; $[(0, \bar{y}, \frac{3}{4}); (3)]$; $[(\frac{1}{2}, \frac{1}{2}-y, \frac{3}{4}); (4)]$
(with $y = 0.4184 \pm 13$).

Bond	Cu(2)–O–Cu(3)	Cu(1)–O–Cu(4)	Cu(2)–O–Cu(4)	Cu(2)–O–Cu(5)
Angle	145.82°	108.85°	104.03°	95.72°
Exchange	J_3	J_4	J_1	J_2

work of Anderson (1950) that the strength of the superexchange coupling displays directional properties, with a maximum for a direct coupling through the O^{2-}. This indicates that in our case the Cu(2)–O–Cu(3) coupling, even if not equal to 180° (see figure 1 and table 1), may be more powerful than the three others.

An antiferromagnetic phase transition in CuO was first briefly reported by Brockhouse (1954) after a powder neutron diffraction experiment. Much later Forsyth *et al* (1988) published a single-crystal neutron diffraction study summarized in table 2. It appeared then that an incommensurate antiferromagnetic structure forms below 232.5 K (phase II), creating in the vicinity of each allowed nuclear peak two first-order satellites defined by the propagation vector $k = 0.506a^* - 0.483c^*$ no higher-order satellites have been observed yet. The positions of the satellites were reported to remain constant in temperature down to the magnetic phase transition at 212.7 K. Below this latter temperature, the structure is commensurate antiferromagnetic with a propagation vector $k = 0.5a^* - 0.5c^*$ (phase I). It is constituted of pairs of ferromagnetic sheets, parallel to the plane $(b, a+c)$.

When analysing the dynamic magnetic properties of CuO (unpublished work) it appeared that the magnetic couplings in this compound were indeed of the particular type that produce helimagnetism, i.e. strong antiferromagnetic interactions along next-

Table 2. Magnetic structure of CuO in both phases, as proposed by several workers.

Phase	(I) commensurate	(II) incommensurate
Temperature	$0 \rightarrow 212.7$ K	$212.7 \rightarrow 232.5$ K
Propagation vector	$\boldsymbol{k} = (\frac{1}{2}, 0, -\frac{1}{2})$	$\boldsymbol{k} = (0.506, 0, -0.483)$
	Data of Forsyth *et al* (1988)	
Magnetic moments	Collinear to b^*	In plane (a^*, c^*)
Structure	↑↑↓↓	Helical
Envelope	Square wave	Elliptical
	Data of Brown *et al* (1991)	
Magnetic moments	Collinear to b^*	In a plane $//b^*$, making[a] an angle of 28.2(8)° with [001]
Structure	↑↑↓↓	Helical
Envelope	Square wave	nearly circular; ellipticity of 1.03
	Present work	
Magnetic moments	Collinear to b^*	In plane[a] $(b^*, 0.506a^* + 1.517c^*)$
Structure	↑↑↓↓	Helical
Envelope	Square wave	Nearly circular; ellipticity of 1±0.05

[a] Plane $(b^*, 0.506a^* + 1.517c^*)$ makes an angle of 28.31° with [001], which is to be compared with the angle of 28.2(8)° found by Brown *et al* (1991).

nearest-neighbours (NNN) bonds Cu(2)–O–Cu(3) (see figure 1 and table 1), hence defining the general direction in which the helical structure will tend to propagate.

The natural pitch angle of this incommensurate structure is given by $\theta_{ij} = 2\pi \boldsymbol{k} \cdot \boldsymbol{r}_{ij}$, where $\boldsymbol{r}_{ij}$ is the vector connecting two copper nearest neighbours (NN) i and j. For couples [(2);(1)], [(2);(4)], [(3);(1)] and [(3);(4)], we have

$$\theta_{21} = \theta_{34} = 86.94° \qquad \theta_{31} = \theta_{24} = 91.08°.$$

It is intuitively understandable that, when the NN coupling of the helimagnetic structure is strong, the pitch angle will approach 0° or 180° depending on whether this coupling is ferromagnetic or antiferromagnetic. Conversely, if this same coupling loosens, the pitch angle is expected to approach 90°. Therefore, the above values for θ_{ij} suggest that the NN exchange couplings are much weaker than the NNN coupling.

It is also clear from the low-temperature collinear arrangement of phase I that b is the easy axis; it corresponds to a magnetic anisotropy responsible for the gap of nearly 0.2 THz (nearly 9 K) in the dispersion curves of magnons, as measured by Aïn *et al* (1989) at $T = 30$ K. Let us emphasize that direction b is a resulting compromise between the two sets of local anisotropy directions, each attached to one set of ribbons. The dipolar anisotropy is very small and will not be considered. This is all the more justified here, as copper has a very small magnetic moment and as all temperatures under consideration are high.

At the incommensurate–commensurate transition, the crystalline anisotropy conveniently aligns all the magnetic moments. The directions of the magnetic moments on NNN couples Cu(2) and Cu(3) are slightly reoriented from 178° to 180°, unlike the moments on NN couples that are subjected to a drastic reorientation from a θ_{24} (or θ_{21}) of 91.06° (or 86.94°), to 0°, showing unambiguously that the NN super-

exchange couplings are weak in CuO. These views were expressed at the 'Réunion IRF—Supraconducteurs à Hautes T_c' held in Grenoble on 15–16 June 1989.

2. Experiment

A polarized neutron experiment was performed on the G6.1 spectrometer at the Orphée reactor of the Laboratoire Léon Brillouin at Saclay to verify some aspects of the magnetic structure of CuO. The wavelength $\lambda = 4.7174$ Å was obtained from a vertically bent graphite monochromator and the incident beam was filtered for the $\lambda/2$ by a block of cooled beryllium. The polarizer and analyser were two Co–Ti benders of Institut Laue–Langevin type. Polarized neutrons were guided by a vertical magnetic field of 20 Oe from the polarizer to the analyser, and through the sample as well. When needed, the spins of the diffracted neutrons were reversed by a flipper coil at the entry of the analyser, with a flip ratio of 70 to 1. It is recalled that the neutron only 'sees' the component $S_\perp$ of the magnetic moment projected on a plane perpendicular to the diffraction vector q. This component, in turn, has to be decomposed into two parts: one parallel to the spin of the neutron and the other perpendicular to it, these latter two components being responsible, respectively, for the non-spin-flip and spin-flip diffraction of the neutron.

The CuO single crystal of 12 mm × 3 mm × 4 mm dimensions was grown by Wanklyn and Garrard (1983) at the Clarendon Laboratory by flux growth in a platinum crucible. The starting materials for the flux were MoO_3, V_2O_3 and K_2CO_3. Its largest dimension was approximately along $a^* + c^*$.

The crystal was oriented with its a^* and c^* axes in the diffraction (horizontal) plane and hence with b^* parallel to the vertical polarization of the neutrons. Therefore, only $(h,0,l)$ Bragg peaks were accessible. In the following we shall be concerned with $(\frac{1}{2},0,\frac{1}{2})$ and $(\frac{1}{2},0,\frac{3}{2})$ reflections, which form an angle of 104.8° in reciprocal space. In the incommensurate region these two peaks shift a little and can be indexed as (0.506, 0, −0.483) and (0.506, 0, 1.517).

The experiment consisted in stabilizing the temperature at selected values in both commensurate and incommensurate regions, pointing successively to the two selected Bragg peaks, and performing rotations of the detector (or θ scan) once with the flipper on and a second time with the flipper off. Table 2 summarizes our observations and those of Brown *et al* (1991), and figure 2 demonstrates this. The peaks in figures 2(*a*) and 2(*b*) were obtained in the commensurate phase at 14.87 K; they show that along two nearly perpendicular directions there is no spin-flip signal, and hence that in phase I all the moments were aligned along b (or b^*). The peaks in figures 2(*c*) and 2(*d*) were obtained in the incommensurate phase II at 221 K. Figure 2(*c*) shows that the spin-flip and non-spin-flip intensities are similar, indicating that the two components of $S_\perp$ already defined, that are seen in the $0.506a^* - 0.483c^*$ direction, are nearly equal. Figure 2(*d*) reveals finally that, in phase II, the peak (0.506, 0, 1.517) is entirely non-spin-flip, proving firstly that the only moment that the neutron 'sees' is parallel to its polarization, confirming that there is indeed a component of the magnetic moment along b (or b^*) as expected, and secondly that the helix is, to a good approximation, in plane (b^*; $0.506a^* + 1.517c^*$), for the reason that the 'invisible' component of the magnetic moment has to be along the diffraction vector q.

Least-squares refinement of the data shows that the plane of the helix is parallel to b^* (or b), and that it makes an angle of $106.9 \pm 1°$ with the propagation vector

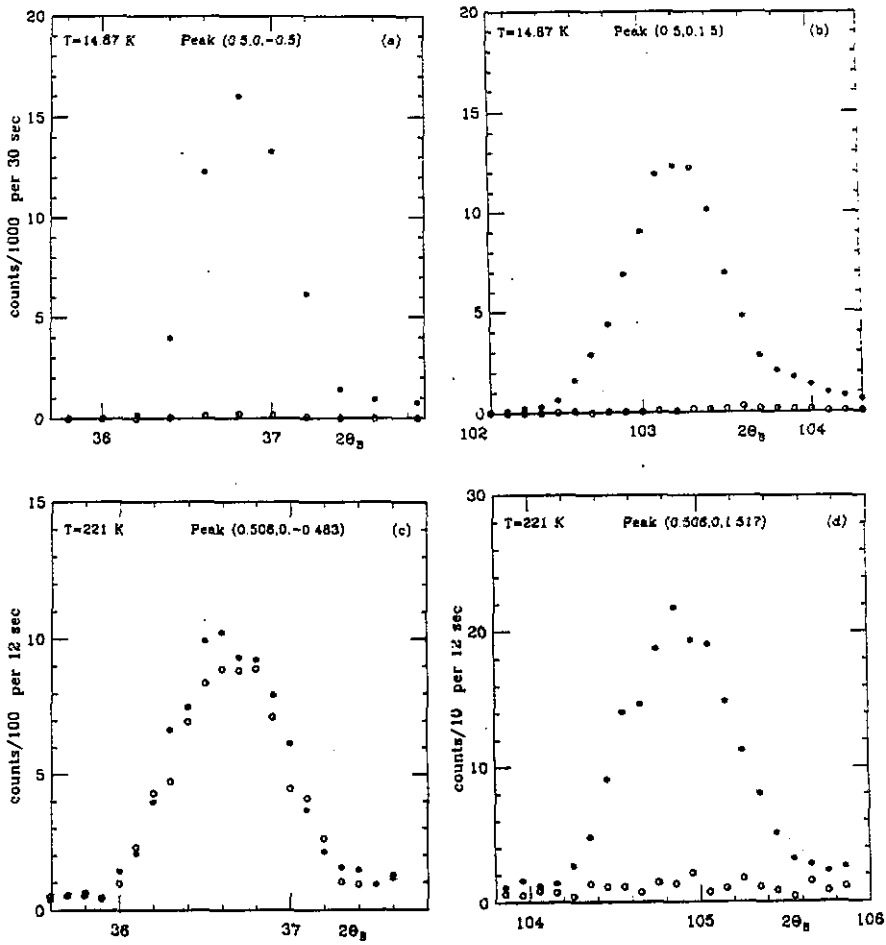

Figure 2. The CuO peaks at $\lambda = 4.717$ Å. *: the spin-flip and O: the non-spin-flip intensities.

$k = 0.506a^* - 0.483c^*$ and $28.19 \pm 1°$ with [001] in β obtuse. It is very close to plane (b^*; $0.506a^* + 1.517c^*$) that makes an angle of 106.78° with the propagation vector and $28.31 \pm 1°$ with [001] in β obtuse. These values are in agreement with the result of Brown *et al* (1991) who have measured an angle of 28.2(8)° between the plane of the helix and [001] in β obtuse, which gives an angle of 106.89(8)° with the propagation vector. It has also been deduced from the data that the envelope of the helix is circular within an error of 5%, this result being in agreement with the work of Brown *et al* (1991). In section 3.1 we shall show that the occurrence of the propagation vector in plane (a^*, c^*) imposes a circular envelope.

Although the crystal was not twinned and revealed a very fine mosaic during triple-axis measurements we should note that the peaks in figure 2 have an irregular shape. This feature will not be discussed here; we simply wish to mention that it has also been observed for nuclear peaks at room temperature in the high-resolution x-ray measurements by Langford and Louër (1991) and is attributed to a distribution in the dimensions of the unit cell and hence to the Cu–O bond lengths. This feature could very well be reflected by a distribution of the superexchange couplings between

copper ions producing the irregular shape of the peaks in phase II.

To compare our measurements with those of Forsyth *et al* (1988), we calculated, at $T = 15$ K, the integrated intensity of each of the two peaks $(\frac{1}{2}, 0, \frac{1}{2})$ and $(\frac{1}{2}, 0, \frac{3}{2})$; the ratio of the corresponding structure factors was found to be

$$F_1/F_2 = \sqrt{(I_1 \sin\theta_1)/(I_2 \sin\theta_2)} = 1.4$$

where the indices $1 \equiv (\frac{1}{2}, 0, \frac{1}{2})$ and $2 \equiv (\frac{1}{2}, 0, \frac{3}{2})$, with θ_i being the corresponding Bragg angle. This result is within 5% of the corresponding ratio obtained from the data in table 2 of Forsyth *et al* (1988).

3. Analysis

Classical theories have been of great help to gain insight into a magnetic structure where an intuitive guess of the arrangements of the magnetic moments is impossible. In section 3.1, the analysis is inspired by the work of Bertaut (1974), Villain (1959) and Yoshimori (1959) (see also Rossat-Mignot (1987) for a review and Regnault and Rossat-Mignot (1990)). Section 3.2 is an application to CuO, of the symmetry analysis of magnetic structures by Bertaut (1968, 1971, 1981).

3.1. Minimizing the Hamiltonian

Every copper ion is coordinated to four oxygen ions, each in turn being coordinated to three other copper ions. However, the total number of neighbours to a particular copper ion is not 12, as expected, but only ten, for the simple reason that successive copper ions on a chain are connected by two different oxygen ions, as is clearly visible in figure 1 (for example: Cu(2) and Cu(5)). The neighbourhood pointers labelled δ_1 to δ_6 are defined in table 3; they are vectors connecting one particular copper ion with the neighbours with which it has a superexchange coupling via an oxygen ion. The first four are common to sites Cu_I and Cu_{II}, while δ_5 and δ_6 are specific and distinctive for sites Cu_I and Cu_{II}, respectively.

Table 3. Row 1: label of neighbourhood pointers; row 2: their definition; row 3: the sites connected; row 4: the corresponding exchange coupling.

Row 1	δ_1	δ_2	δ_3	δ_4	δ_5	δ_6
Row 2	$(a+c)/2$	$(c+b)/2$	$(c-b)/2$	$(a-c)/2$	$(b+a)/2$	$(b-a)/2$
Row 3	Cu_I–Cu_{II}	Cu_I–Cu_{II}	Cu_I–Cu_{II}	Cu_I–Cu_{II}	Cu_I–Cu_I	Cu_{II}–Cu_{II}
Row 4	J_4	J_1	J_1	J_3	J_2	J_2

We shall proceed with the minimization of the Hamiltonian to the point necessary to the needs of understanding the static magnetic structure, postponing a more complete development to a forthcoming paper on spin waves in CuO. As a preliminary, we have to select the interactions that will be included in the Hamiltonian. The anisotropy term will be absent in the expression for the Hamiltonian, because the experimental results do not display its signature. Anisotropy produce a distortion of the regular arrangement of the helix, and one would expect to observe high-order satellites among the magnetic diffraction peaks (Coqblin 1977, Jensen and Mackintosh 1991), which has not been the case to date. Hence the remainder of this section

applies to the incommensurate phase where an anisotropy term is irrelevant. It is merely responsible for the orientation of the plane of the helix.

Summing separately over all sites Cu_I and Cu_{II}, the Hamiltonian reads

$$H = \tfrac{1}{2}\sum_{i\in Cu_I}\sum_{\mu} J(\delta_\mu)S(r_i)\cdot S(r_i+\delta_\mu) + \tfrac{1}{2}\sum_{i\in Cu_{II}}\sum_{\nu} J(\delta_\nu)S(r_j)\cdot S(r_j+\delta_\nu) \tag{1}$$

where δ_μ and δ_ν belong to the set $\{\pm\delta_1 \ldots \pm\delta_6\}$.

When a magnetic structure generates two first-order satellites $\pm k$ around each nuclear peak, it implies that the Fourier transform of the spin operator on site r reduces to

$$S(r_i) = S_I(k)\exp(i2\pi k\cdot r_i) + S_I(-k)\exp(-i2\pi k\cdot r_i) \qquad \text{for sites } Cu_I \tag{2a}$$

$$S(r_j) = S_{II}(k)\exp(i2\pi k\cdot r_j) + S_{II}(-k)\exp(-i2\pi k\cdot r_j) \qquad \text{for sites } Cu_{II} \tag{2b}$$

with $S_I(k) = S_I(-k)^*$ and $S_{II}(k) = S_{II}(-k)^*$. In order to check that the amplitudes of moments on equivalent sites are equal, we have to write that

$$|S(r_i)|^2 = S_I(k)^2\exp(i4\pi k\cdot r_i) + S_I(k)^2\exp(-i4\pi k\cdot r_i) + 2S_I(k)\cdot S_I(-k)$$
$$\equiv S_I^2 \qquad \text{for } Cu_I \tag{3a}$$

$$|S(r_j)|^2 = S_{II}(k)^2\exp(i4\pi k\cdot r_j) + S_{II}(k)^2\exp(-i4\pi k\cdot r_j) + 2S_{II}(k)\cdot S_{II}(-k)$$
$$\equiv S_{II}^2 \qquad \text{for } Cu_{II} \tag{3b}$$

where spins on inequivalent sites are not supposed equal, i.e. S_I is not necessarily equal to S_{II}. We can easily see that, if k is incommensurate, equations (3) can be satisfied only if the factors of the exponentials are zero. This is verified if $S_I(k)$ and $S_{II}(k)$ are two vectors proportional to $(u-iv)$, u and v being two unitary orthogonal vectors. One then has $S_I(k)^2 = 0$ and $S_{II}(k)^2 = 0$, hence cancelling the terms with exponentials.

Replacing equations (2) in the Hamiltonian (1) gives

$$H = N\{\zeta_1[S_I(k)\cdot S_{II}(-k) + S_I(-k)\cdot S_{II}(k)] + \zeta_2 S_I(k)\cdot S_I(-k)$$
$$+ \zeta_3 S_{II}(k)\cdot S_{II}(-k)\} \tag{4}$$

where N is the number of copper ions on each site and

$$\zeta_1 = J_4\cos(2\pi k\cdot\delta_1) + J_1[\cos(2\pi k\cdot\delta_2) + \cos(2\pi k\cdot\delta_3)] + J_3\cos(2\pi k\cdot\delta_4) \tag{5a}$$

$$\zeta_2 = J_2\cos(2\pi k\cdot\delta_5) \tag{5b}$$

$$\zeta_3 = J_2\cos(2\pi k\cdot\delta_6). \tag{5c}$$

The minimization of the Hamiltonian (4) relatively to $S_I(k)$ and $S_{II}(k)$ is subjected to the constraint relations (3). Without loss of generality we can begin with a weaker

condition, ensuring solely that the sum of all the squared amplitudes of the magnetic moments on both sites be fixed. This is obtained by adding equations (3*a*) and (3*b*):

$$\sum_{i\in Cu_I} S_I(k)\cdot S_I(-k) + \sum_{j\in Cu_{II}} S_{II}(k)\cdot S_{II}(-k) = N(S_I^2 + S_{II}^2) = \text{constant}. \tag{6}$$

Now applying the Lagrange multiplier technique to minimize equation (4) submitted to the constraint (6) leads to the equations

$$\zeta_1 S_{II}(k) + \zeta_2 S_I(k) = \lambda S_I(k) \tag{7a}$$

$$\zeta_3 S_{II}(k) + \zeta_1 S_I(k) = \lambda S_{II}(k) \tag{7b}$$

where λ is the Lagrange multiplier. Equations (7) admit non-trivial solutions only if

$$\lambda = \tfrac{1}{2}\left\{(\zeta_2+\zeta_3) \pm [(\zeta_2-\zeta_3)^2 + 4\zeta_1^2]^{1/2}\right\}$$

in which case the amplitudes of the magnetic moments on sites Cu_I and Cu_{II} are related by

$$S_{II}(k) = [(\lambda-\zeta_2)/\zeta_1]S_I(k) = [\zeta_1/(\lambda-\zeta_3)]S_I(k) = \Gamma S_I(k).$$

Thus we reach an important result for CuO, namely, if $\Gamma = 1$, that is to say if we have equal moments on sites Cu_I and Cu_{II}, then we must have $\zeta_2 = \zeta_3$ or equivalently from (5*b*) and (5*c*)

$$\cos(2\pi k\cdot\delta_5) = \cos(2\pi k\cdot\delta_6). \tag{8}$$

Conversely examination of condition (8) shows that, if the propagation vector k is confined to plane $(b, a\times b)$ or to plane (a, c) where it actually lies, then we can conclude that the amplitude of the magnetic moments on sites Cu_I and Cu_{II} are equal. As a corollary this imposes a circular envelope to the helical structure. The occurrence of k in either plane depending on the particular values of the $(J_1 \ldots J_4)$.

3.2. Symmetry arguments

With the knowledge of the propagation vector $k = (k_x, k_y, k_z)$ for the magnetic structure and the direction of the magnetic moments in CuO, we can derive the different magnetic configurations compatible with the magnetic space group G_k of CuO; this is readily obtained from a symmetry analysis of the magnetic representations (Bertaut 1968, 1971, 1981).

The underlying point group of $C2/c$ is $C_{2h}(2/m) = \{1, 2_y, \bar{1}, m\}$. The propagation vector k of the magnetic phase of CuO is invariant under the glide plane $\mathbf{c} = \{m_y|0,0,\frac{1}{2}\}$, but not under the twofold axis 2_y, hence reducing the point group to $C_{1h}(m) = \{1, m\}$, and the magnetic space group G_k to Cc (No 9). We can choose as generators of space group Cc the three primitive translations, plus $\mathbf{C} = \{1|\frac{1}{2},\frac{1}{2},0\}$, a non-primitive translation, and $\mathbf{c}$. Therefore we have the coset expansion

$$G_k = 1T + \mathbf{C}T + \mathbf{c}T + (\mathbf{Cc})T$$

where T is the invariant subgroup of the primitive translations. In the following we shall choose the reference copper ions at:

$$[(\tfrac{1}{4},\tfrac{1}{4},0),\mathrm{Cu}(1)] \qquad [(\tfrac{3}{4},\tfrac{3}{4},0),\mathrm{Cu}(2)] \qquad [(\tfrac{1}{4},\tfrac{\bar{1}}{4},\tfrac{1}{2}),\mathrm{Cu}(3)] \qquad [(\tfrac{3}{4},\tfrac{1}{4},\tfrac{1}{2}),\mathrm{Cu}(4)]$$

in preference to those in table 1. The transformation matrices for the y component of the Fourier transform of the magnetic moment are deduced from the following relations:

$$\mathbf{C}S^k_{1y} = S^k_{2y} \qquad \mathbf{C}S^k_{2y} = a^2 S^k_{1y} \qquad (1,1,0) \qquad (9a)$$

$$\mathbf{C}S^k_{3y} = S^k_{4y} \qquad \mathbf{C}S^k_{4y} = a^2 S^k_{3y} \qquad (1,1,0) \qquad (9b)$$

$$\mathbf{c}S^k_{1y} = S^k_{3y} \qquad \mathbf{c}S^k_{2y} = S^k_{4y} \qquad (0,1,0) \qquad (9c)$$

$$\mathbf{c}S^k_{3y} = b^2 S^k_{1y} \qquad (0,0,1) \qquad \mathbf{c}S^k_{4y} = b^2 S^k_{2y} \qquad (0,1,1) \qquad (9d)$$

where in parentheses we have written the primitive translation involved in the transformation, and where $a^2 = \exp(\mathrm{i}2\pi k_x)$ and $b^2 = \exp(\mathrm{i}2\pi k_z)$. When dealing with a component parallel to the glide plane (called the in-plane component), one will simply have to reverse the signs of all the right-hand sides in equations (9c) and (9d).

In matrix form equations (9) read

$$\mathbf{C} = \begin{bmatrix} 0 & 0 & 1 & 0 \\ 0 & 0 & 0 & 1 \\ a^2 & 0 & 0 & 0 \\ 0 & a^2 & 0 & 0 \end{bmatrix} \qquad \mathbf{c} = \begin{bmatrix} 0 & 0 & 1 & 0 \\ 0 & 0 & 0 & 1 \\ b^2 & 0 & 0 & 0 \\ 0 & b^2 & 0 & 0 \end{bmatrix}.$$

These generators satisfy the defining relations that follow:

$$\mathbf{C}^2 = a^2\mathbf{1} \qquad \mathbf{c}^2 = b^2\mathbf{1} \qquad \mathbf{cC} = \mathbf{Cc} = \begin{bmatrix} 0 & 0 & 0 & 1 \\ 0 & 0 & a^2 & 0 \\ 0 & b^2 & 0 & 0 \\ a^2b^2 & 0 & 0 & 0 \end{bmatrix}$$

where $\mathbf{1}$ is the identity operator. These matrices constitute a representation Γ of the problem in hand. Table 4 gives the character table of the irreducible representations of $G_k = Cc$, note that they are one-dimensional.

Table 4. Character table of the irreducible representations of G_k.

	1	Cc	C	c
Γ_1	1	ab	a	b
Γ_2	1	ab	$-a$	$-b$
Γ_3	1	$-ab$	a	$-b$
Γ_4	1	$-ab$	$-a$	b

By application of the projection operator we shall obtain the basis vector of each representation Γ_ν.

$$V_\nu^k = \sum^{\mathbf{h}} d_\nu(\mathbf{h})^* \mathbf{h} V^k$$

where $d_\nu(\mathbf{h})$ is the unique matrix element associated with operator $\mathbf{h}$ in any of the representations Γ_1–Γ_4, and V^k is a linear combination of the S_{iy}^k. Choosing $V^k = S_{1y}^k$, one finds that

$$\begin{aligned}
V_1^k &= S_{1y}^k + a^* b^* S_{4y}^k - a^* S_{2y}^k - b^* S_{3y}^k \\
V_2^k &= S_{1y}^k + a^* b^* S_{4y}^k + a^* S_{2y}^k + b^* S_{3y}^k \\
V_3^k &= S_{1y}^k - a^* b^* S_{4y}^k - a^* S_{2y}^k + b^* S_{3y}^k \\
V_4^k &= S_{1y}^k - a^* b^* S_{4y}^k + a^* S_{2y}^k - b^* S_{3y}^k .
\end{aligned}$$

Only one vector at a time can contribute to each component of the magnetic moment (Bertaut 1981). Choosing $V_1^k \neq 0$ and $V_2^k = V_3^k = V_4^k = 0$ for example, we obtain

$$S_{1y}^k = \tfrac{1}{4} V_1^k \qquad S_{2y}^k = -\tfrac{1}{4} a V_1^k \qquad S_{3y}^k = -\tfrac{1}{4} b V_1^k \qquad S_{4y}^k = \tfrac{1}{4} ab V_1^k .$$

Let us write $V_1^k = 2S_0 \exp(\mathrm{i}2\pi\varphi)$, where φ is an adjustable parameter. Then, in the representation Γ_1, we can express the magnetic moment on each copper ion inside cell i as (see relations (I-4)–(I-6) of Bertaut (1971))

$$\begin{aligned}
S_{1y}^i &= S_0 \cos(2\pi \boldsymbol{k} \cdot \boldsymbol{r}_i + \varphi) \\
S_{2y}^i &= -S_0 \cos[2\pi(\boldsymbol{k} \cdot \boldsymbol{r}_i + k_x/2) + \varphi] \\
S_{3y}^i &= -S_0 \cos[2\pi(\boldsymbol{k} \cdot \boldsymbol{r}_i + k_z/2) + \varphi] \\
S_{4y}^i &= S_0 \cos\{2\pi[\boldsymbol{k} \cdot \boldsymbol{r}_i + (k_x + k_z)/2] + \varphi\}.
\end{aligned} \tag{10}$$

In the commensurate phase I, we have

$$k_x = \tfrac{1}{2} \qquad k_z = -\tfrac{1}{2} \qquad a = i \qquad b = -i.$$

Furthermore the parameter φ has to be set to $\pi/4$, in order that all moments on sites Cu_I and Cu_{II} have equal amplitude as desirable from section 3.1 (condition (8)); then the arrangement is such as ↑↑↓↓, Cu(1) and Cu(4) being parallel, and Cu(2) and Cu(3) antiparallel. We can verify that selecting $V_2^k \neq 0$ rather than V_1^k gives the same configuration. If V_3^k (or V_4^k) $\neq 0$ then Cu(1) and Cu(4) are antiparallel, and Cu(2) and Cu(3) are parallel, but this configuration is totally unacceptable, with respect to the measured intensities of the magnetic Bragg peaks.

In the incommensurate phase II, we have, for the y component, the same relations (10) pertaining to representation Γ_1, and for the in-plane component with the same representation we have

$$\begin{aligned}
S_{1p}^i &= S_0 \cos(2\pi \boldsymbol{k} \cdot \boldsymbol{r}_i + \varphi_p) \\
S_{2p}^i &= -S_0 \cos[2\pi(\boldsymbol{k} \cdot \boldsymbol{r}_i + k_x/2) + \varphi_p] \\
S_{3p}^i &= S_0 \cos[2\pi(\boldsymbol{k} \cdot \boldsymbol{r}_i + k_z/2) + \varphi_p] \\
S_{4p}^i &= -S_0 \cos\{2\pi[\boldsymbol{k} \cdot \boldsymbol{r}_i + (k_x + k_z)/2] + \varphi_p\}
\end{aligned} \tag{11}$$

with $\varphi = 0$ in (10) and $\varphi_p = \pi/2$ in (11) to satisfy condition (8). Here again equations (10) and (11) describe the observed helical structure with a circular envelope.

4. Conclusion

It is not a common practice to use neutron polarization analysis to study magnetic structure, and yet we have proved that it can be a decisive technique. There is agreement between us and Brown *et al* (1991) who have used a more sophisticated technique. We both find the same propagation vector $k = (0.506, 0, -0.483)$ for the helical structure of the incommensurate phase. The plane of the helix is parallel to b^* (or b) and makes an angle of $106.9 \pm 1°$ with the propagation vector and $28.19 \pm 1°$ with [001] in β obtuse, to be compared with the value of 28.2(8)° found by Brown *et al* (1991). Finally, we both found a nearly circular envelope for the helix.

In the theoretical part of the paper we neglect the anisotropy term in the Hamiltonian describing the incommensurate phase of CuO. This is justified by the absence of high-order satellites. We show then that in the minimization process of the Hamiltonian a constraint appears, which imposes the condition that the envelope of the helix should be circular if the propagation vector is found in plane $(b, a \times b)$ or in plane (a, c) where it actually lies.

Acknowledgments

We gratefully thank O Guiselin for his help with the algebra, and P Calmettes for discussions on CuO and on polarized-neutron topics. We also thank B Coqblin for illuminating discussions.

Note added in proof. Åsbrink and Wáskowska (1991) suggest that in a new refinement of a new x-ray experiment on CuO, the correct space group could be *Cc* as it is proposed in this paper for the magnetic system.

References

Aïn M, Reichardt W, Hennion B, Pépy G and Wanklyn B M 1989 *Physica* C **162–4** 1279–80
Anderson P W 1950 *Phys. Rev.* **79** 350
Åsbrink S and Norrby L-J 1970 *Acta Crystallogr.* B **26** 8
Åsbrink S and Wáskowska A 1991 *J. Phys.: Condens. Matter* **3** 8173–80
Bertaut E F 1968 *Acta Crystallogr.* A **24** 217
—— 1971 *J. Physique Coll.* **32** C1 462
—— 1974 *J. Physique* **35** 659–77
—— 1981 *J. Magn. Magn. Mater.* **24** 267–78
Brockhouse B N 1954 *Phys. Rev.* **94** 781
Brown P J, Chattopadhyay T, Forsyth J B, Nunez V and Tasset F 1991 *J. Phys.: Condens. Matter* **3** 4281–7
Coqblin B 1977 *The Electronic Structure of Rare-Earth Metals and Alloys: the Magnetic Heavy Rare-Earths* (New York: Academic) pp 130, 162
Forsyth J B, Brown P J and Wanklyn B M 1988 *J. Phys. C: Solid State Phys.* **21** 2917 1279–80
Jensen J and Mackintosh A R 1991 *Rare Earth Magnetism* (Oxford: Clarendon) p 81
Langford J I and Louër D 1991 *J. Appl. Crystallogr.* **24** 149–55
Regnault L P and Rossat-Mignot J 1990 *Magnetic Properties of Layered Transition Metal Compounds* ed L J De Jongh (Deventer: Kluwer) pp 271–321
Rossat-Mignot J 1987 *Methods of Experimental Physics* vol 3, part C (New York: Academic) pp 69–157
Villain J 1959 *J. Phys. Chem. Solids* **11** 303
Wanklyn B M and Garrard B J 1983 *J. Mater. Sci. Lett.* **2** 285
Yang B X, Thurston T R, Tranquada J M and Shirane G 1989 *Phys. Rev.* B **39** 4343
Yang B X, Tranquada J M and Shirane G 1988 *Phys. Rev.* B **38** 174
Yoshimori A 1959 *J. Phys. Soc. Japan* **14** 807–21